SYNTHESIS AND STRUCTURAL CHARACTERIZATION OF LaMnO$_{3+\delta}$ AND La$_{0.8}$AE$_{0.2}$MnO$_{3+\delta}$ (AE=Ca, Sr, Ba) PEROVSKITES FOR CATALYTIC OXIDATION OF VOLATILE ORGANIC COMPOUNDS

Natasha Di Benedetto[a], Carolina de los Santos[b], Alejandro Amaya[b], Leopoldo Suescun[a],*, Jorge Castiglioni[b],*.

[a] *Laboratorio de Cristalografía, Química del Estado Sólido y Materiales/DETEMA/Facultad de Química/Universidad de la República, Montevideo, Uruguay*

[b] *Laboratorio de Fisicoquímica de Superficies/Área Fisicoquímica/DETEMA/Facultad de Química/Universidad de la República, Montevideo, Uruguay*
E-mail: leopoldo@fq.edu.uy, jcastiglioni@fq.edu.uy

Resumen

Las perovskitas LaMnO$_3$ y La$_{0.8}$AE$_{0.2}$MnO$_3$ (AE=Ca, Sr, Ba) fueron preparadas en un único paso mediante el método de autocombustión y caracterizadas mediante difracción de rayos X y fisisorción de nitrógeno, para su aplicación como catalizadores en la oxidación completa de compuestos orgánicos volátiles. Las fases estudiadas presentan las estructuras cristalinas tipo perovskita esperadas (ortorrómbica y romboédrica). Los materiales obtenidos directamente de la síntesis (cenizas) son óxidos estequiométricos que durante un pre-tratamiento de calcinación a 750 °C se transforman irreversiblemente en estructuras con vacancias de cationes de fórmula LaMnO$_{3+\delta}$ y La$_{0.8}$AE$_{0.2}$MnO$_{3+\delta}$. Las áreas específicas (método BET) fueron determinadas para las muestras en forma de polvo antes de la evaluación catalítica, mostrando valores bajos pero acordes a lo esperado para polvos microparticulados. En los experimentos de catálisis se pudo apreciar que casi no existe relación entre el estado inicial o el metal alcalinotérreo presente en el material y la performance obtenida. Mediante experimentos de termo-difracción in situ se pudo comprobar que las cenizas, fases estequiométricas, empiezan a convertirse en fases deficientes en cationes entre los 200 y 300 °C. Esto sugiere que el factor más importante para la actividad catalítica de estos óxidos, sino el único, es el cociente molar Mn^{4+}/Mn^{3+} en la superficie de las muestras.

Palabras clave: VOC, perovskitas, catálisis, acetona

Abstract

Perovskites LaMnO$_3$ and La$_{0.8}$AE$_{0.2}$MnO$_3$ (AE=Ca, Sr, Ba) have been prepared by a simple one-step auto-combustion method and were characterized by X-ray powder diffraction and N$_2$ adsorption-desorption method in order to apply them as catalysts in the complete catalytic oxidation of volatile organic compounds. The studied phases show the expected orthorhombic and rhombohedral perovskite crystal structures, being as-prepared materials stoichiometric oxides that transform irreversibly into cation deficient LaMnO$_{3+\delta}$ and La$_{0.8}$AE$_{0.2}$MnO$_{3+\delta}$ during a pre-treatment of calcination at 750 °C. BET areas were determined for the powders before catalytic experiments and are low but expected for ground microparticulate powders. The catalytic experiments show almost no dependence on the state of the initial sample or AE cation. As-prepared stoichiometric samples slowly convert to cation deficient phases between 200 and 300 °C as supported by in-situ thermo-diffraction experiments. This suggests that the most important factor for the activity of these oxides as catalysts, if not the only one, is the Mn^{4+}/Mn^{3+} molar ratio in the surface of the samples.

Keywords: VOC, perovskites, catalysis, acetone

SI estamos dispuestos a someter nuestro trabajo al volumen especial dedicado al CICAT 2020 en caso de que sea seleccionado por los revisores y el comité científico.

1. Introduction

Volatile organic compounds (VOCs) are a group of carbon-based chemicals considered not only as major contributors to air pollution but also one of the main hazardous substances for human health. Due to the great impact they provoke, the scientific community has been in search of an economically viable solution in order to control VOCs emissions.

A few decades ago, the catalytic oxidation process arose as an interesting alternative to previously proposed methods, because it achieves greater conversions to CO_2 and H_2O at lower temperatures, is easier to control and less expensive in the long term. An additional complication of VOCs is that these group includes a wide range of compounds with very different physicochemical properties, what makes it difficult to find a single catalyst for the effective elimination of the majority of them.[1-3]

Transition metal oxides, specially manganites, have been tested for VOCs oxidation and proved active at low temperatures for several molecules. Among them, manganites with perovskite-like structure are the ones that have exhibited the best performances. This can be attributed to the redox properties of the manganese and the mobility of oxygen in the lattice.[4-8]

In this work, mesoporous, stoichiometric $LaMnO_3$ and AE substituted $La_{0.8}AE_{0.2}MnO_3$ (AE=Ca, Sr, Ba) perovskites were prepared, structurally characterized and tested as catalysts in the complete combustion of acetone (chosen as model VOC). The effects of different alkaline-earth metals substitution and the differences between the as prepared/calcined samples on the catalytic results are presented.

2. Experimental

2.1. Catalysts preparation

$LaMnO_3$ and $La_{0.8}AE_{0.2}MnO_3$ (AE= Ca, Sr, Ba), perovskites were synthesized via an auto-combustion route, using ethylenediamine-tetraacetic acid (EDTA, $C_{10}H_{16}N_2O_8$) as fuel and chelating agent and ammonium nitrate (NH_4NO_3) as combustion promoter [9]. Aqueous solutions containing the metals were prepared employing stoichiometric quantities of La, Sr and Ba nitrates and Mn and Ca acetates (>99.9 %, Sigma-Aldrich), according to the desired composition. An alkaline solution (pH=10) containing 1.1 mole of EDTA per mole of cation and NH_4NO_3 was also prepared and the aforementioned solutions were added. EDTA molar excess ensures the complete

complexation of the cations. A 1:10 $EDTA:NH_4NO_3$ molar ratio was chosen to promote the auto-combustion process. The resulting solution was heated over a hot plate at 130 °C - constantly stirring and keeping pH constant- until the formation of a gel. The hot plate was taken to 300 °C, where the gel self-ignites forming the desired perovskite compound in a very loose nanostructured powder, as confirmed by X-ray powder diffraction. All of the samples were grinded in an agate mortar and separated in two fractions. The first fraction, of as-prepared samples $LaMnO_3$ (LM), $La_{0.8}Ca_{0.2}MnO_3$ (LCM), $La_{0.8}Sr_{0.2}MnO_3$ (LSM) and $La_{0.8}Ba_{0.2}MnO_3$ (LBM) were characterized and used for the catalytic experiments. The second fraction of each was calcined at 750 °C in air during 8h to obtain $LaMnO_{3+\delta}$ (LM750), $La_{0.8}Ca_{0.2}MnO_{3+\delta}$ (LCM750), $La_{0.8}Sr_{0.2}MnO_{3+\delta}$ (LSM750) and $La_{0.8}Ba_{0.2}MnO_{3+\delta}$ (LBM750) also studied.

2.2. Catalysts characterization

2.2.1. X-ray powder diffraction (XPD)

Conventional X-ray powder diffraction measurements were performed over as-prepared and calcined samples with a Rigaku ULTIMA IV diffractometer using CuKα sealed-tube radiation (λ=1.5418 Å) operating at 40 kV and 30 mA. A diffracted-beam curved Ge monochromator, and scintillation detector were also used for data collection. The data was collected at room temperature in the 2θ=10-70° range in 0.04° steps for 3 s.

The as-prepared samples were also characterized through X-ray thermo-diffraction at the XPD-D10B beamline of the Brazilian Synchrotron Light Laboratory (LNLS), in order to characterize the phase composition of the sample at the conditions of catalysis. The measurements were performed from RT to 700 °C in air atmosphere using the Canario furnace, and X-rays with an energy of 10 keV (λ=1.2372 Å). The beamline is equipped with a θ-2θ reflection-geometry diffractometer with a Mythen 1000 linear position sensitive detector (PSD). Data reduction and averaging was carried out with the in-house software to obtain powder patterns in the 8-120 ° range with 0.005° 2θ-steps. The fit of the data was performed by the Rietveld method using GSAS-II software suite [10], in order to determine the phase composition and structural parameters of the samples.

2.2.2. Specific surface area

Specific surface area (S_{BET}) measurements were performed by the BET method for nitrogen

adsorption isotherms (Praxair, > 99.95 %) at 77 K on outgassed samples during 15 h at 50 °C. The isotherms were registered until relative pressures equal to 0.99 P$_o$ using a Beckman Coulter SA3100 apparatus.

2.2.3. Catalytic evaluation

Catalytic experiments were carried out in a quartz tubular reactor with "u" shape (external diameter=8 mm) using a 0.5 g catalyst sample. A pretreatment of the catalyst was performed at 300 °C for 30 min in Ar flow. The reactivity of the samples was determined at atmospheric pressure, between 100 and 350 °C, with an Ar/O$_2$/Acetone reaction mixture (120 mL min^{-1}, 3.43 mL min^{-1} and 1500 ppm$_v$, respectively). The O$_2$ goes through a saturator containing acetone (>99.5 %, Dorwil), submerged in a water/ice bath and the resulting mixture is diluted in Ar. Quantification of reagents and reaction products was accomplished by gas chromatography on a Shimadzu GC 2014, using a HAYESEP R 60/80 mesh column (diameter 1/8 mm SS, length 4.5 m) and TCD and FID detectors in series.

3. Results and discussion

LaMnO$_3$, and AE doped La$_{0.8}$AE$_{0.8}$MnO$_3$ (AE=Ca, Sr, Ba) perovskite phases have been well known for several decades [11]. When prepared in air at high temperatures, they form metal-vacant phases La$_{1-x}$Mn$_{1-x}$O$_3$ and (La$_{0.8}$AE$_{0.2}$)$_{1-x'}$Mn$_{1-x'}$O$_3$ (x'<x) of rhombohedral symmetry ($R\bar{3}c$ space group) usually described as LaMnO$_{3+\delta}$ and La$_{0.8}$AE$_{0.2}$MnO$_{3+\delta}$ [12] where δ represents excess oxygen respect to the metals, even though the perovskite phases do not allow interstitial non-stoichiometric oxygen in the structure. These metal-vacant phases are stabilized by the oxidation of Mn^{3+} into Mn^{+4} in the presence of oxygen at moderate-to-high temperatures achieving equilibrium with maximum δ=0.26 or 26% of Mn^{4+} for LaMnO$_3$ annealed at 1000 °C in O$_2$.[13] Preparation of oxygen-stoichiometric LaMnO$_3$ and La$_{0.8}$AE$_{0.2}$MnO$_3$ containing pure Mn^{3+} or up to 20% Mn^{4+}, respectively, was usually achieved by firing non-stoichiometric phases at low oxygen-partial-pressure atmosphere [14,15], observing a change in the symmetry of the perovskite structures from the metal-vacant rhombohedral $R\bar{3}c$ structure to the stoichiometric orthorhombic *Pnma*.

The auto-combustion synthesis method used in this work yields pure and oxygen stoichiometric phases in one step. Therefore, we were able to obtain orthorhombic LaMnO$_3$ (LM) (see top panel of Figure 1), La$_{0.8}$Ca$_{0.2}$MnO$_3$ (LCM) and

La$_{0.8}$Sr$_{0.2}$MnO$_3$ (LSM), and mixed-phase orthorhombic and rhombohedral La$_{0.8}$Ba$_{0.2}$MnO$_3$ (LBM). These phases are all oxygen and metal stoichiometric, being the change in the symmetry caused only by the ionic radii of the AE cation that produces a symmetry increase with increase of the average size of the A site, as generally observed with ABO$_3$ perovskites [16].
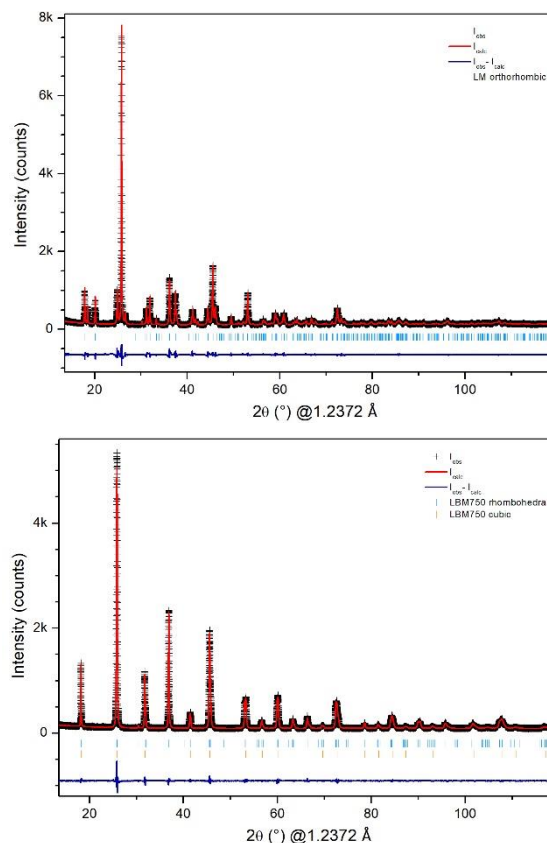

Figure 1. Rietveld fit of synchrotron XPD pattern of LM (**top**) and LBM750 (**bottom**) samples confirming the presence of pure samples with orthorhombic *Pnma* and rhombohedral $R\bar{3}c$ symmetry in the samples used for catalysis experiments. LBM750 sample also contains some ~10% of the cubic $Pm\bar{3}m$ perovskite phase.

Another set of samples, prepared from LM, LCM, LSM and LBM calcined at 750 °C in air was obtained. This changed the oxygen content and symmetry of the as-prepared compounds producing rhombohedral LaMnO$_{3+\delta}$ (LM750), La$_{0.8}$Ca$_{0.2}$MnO$_{3+\delta}$ (LCM750), La$_{0.8}$Sr$_{0.2}$MnO$_{3+\delta}$ (LSM750) and rhombohedral+cubic La$_{0.8}$Ba$_{0.2}$MnO$_{3+\delta}$ (LBM750) (see bottom panel of Figure 1). In all these phases it may be considered that the average Mn oxidation state is the same, since the Mn^{4+}/Mn^{3+} equilibrium dictates the formation of cation vacancies, so even in the

presence of different Mn^{4+}/Mn^{3+} ratio (0 for LM, 0.2 for the others). The final calcined phases should have a larger Mn^{4+} content with a lower amount of cation vacancies in the doped samples [12,15].
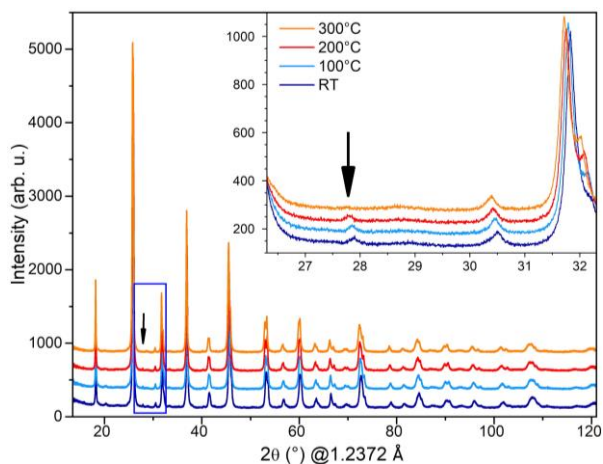

Figure 2. Synchrotron XPD patterns of as-prepared $La_{0.8}Sr_{0.2}MnO_3$ (LSM) heated from RT to 300 °C in air. Note that the peak at ~28 ° almost disappears at 300 °C indicating the oxygen uptake with formation of cation vacancies and irreversible transformation of the orthorhombic to rhombohedral phase.

It is reasonable to say then, that all calcined phases show La/AE/Mn vacancies at all times, while all as-prepared samples show no cation or oxygen vacancies at the beginning of the catalytic tests.
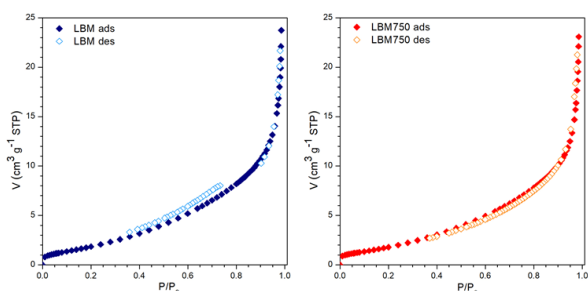

Figure 3. N_2 physisorption isotherms for LBM (**left**) and LBM 750 (**right**) samples.

Nitrogen physisorption isotherms for LBM and LBM750 are shown in Figure 3. According to IUPAC classification, the curves in the figure correspond to a limit case among type III and IV with low adsorption at low relative pressures. The increase of adsorbed amounts at relative pressures among 0.2 y 0.8 evidences the presence of mesopores, and the increase over 0.8 the presence of macropores. In LBM, a small hysteresis (H3 type, Boer) is perceived, what could indicate the presence of lamellar solids. For LBM750, the hysteresis disappears, denoting a slight modification in the porosity of the sample during the calcination process used to transform LBM into LBM750. This behavior is similar in all the doped samples.

The results of textural properties obtained for as-prepared and calcined manganites are shown in Table 1. In general, it is observed that both types of samples have similar specific surface areas (S_{BET}), with really low values, but comparable to those reported in the literature for other perovskites prepared by similar methods [8, 17-20]. A small decrease in specific area can be observed when samples are subjected to calcination -what is consistent with nitrogen adsorption isotherms results- except for LCM750, where the area seems to slightly increase despite having similar total pore volume (V_{total}).

Table 1. Textural properties for as-prepared and calcined maganites.

Catalyst	S_{BET} [$m^2 g^{-1}$]	V_{total} [$m^3 g^{-1}$]
LM	5,7	0,025
LM750	4,7	0,015
LCM	5,0	0,030
LCM750	6,9	0,030
LSM	7,0	0,030
LSM750	5,5	0,030
LBM	7,1	0,030
LBM750	6,7	0,030

Acetone conversion vs temperature curves for the as-prepared and the calcined manganites are shown in Figure 4. All samples show that total conversion of acetone is achieved below 300 °C with a measurable catalytic activity starting between 100 and 150 °C. Both $LaMnO_3$ and AE doped samples

show very similar acetone conversion capability at 250 °C. At 100 °C LM sample is slightly more active than LCM, LSM and LBM but this difference vanishes upon calcination where the four samples LM750, LCM750, LSM750 and LBM750 show 20% conversion at 100 °C and 100% conversion at 250 °C.
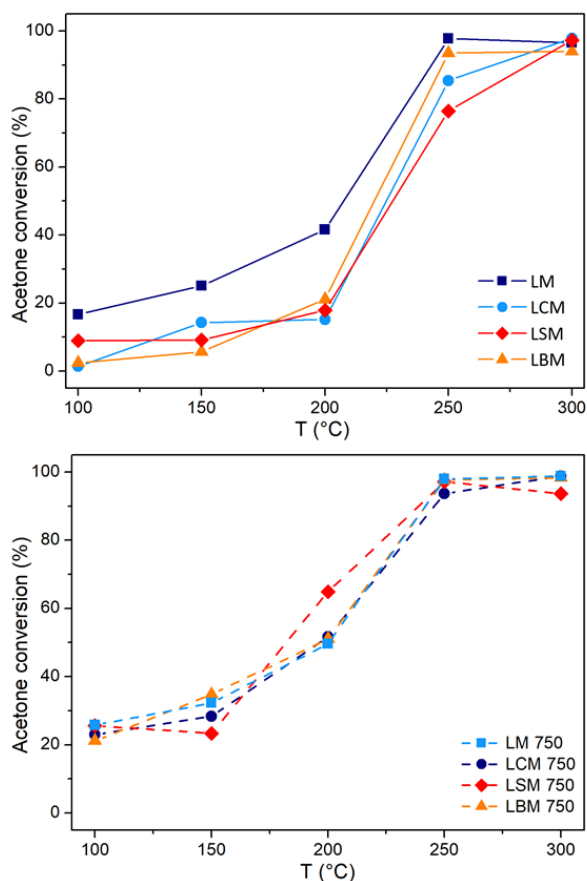

Figure 4. Acetone conversion vs temperature curves for the as-prepared manganites LM, LCM, LSM and LBM (**top**) and the calcined samples LM750, LCM750, LSM750 and LBM750 (**bottom**).

Looking at the light-off curves in more detail, we note that the as-prepared samples show about 20% conversion at 200 °C but the activity increases four-fold (to over 80%) with a small temperature increase of 50 °C. For the calcined samples the change from 20% to 80% conversion runs over a larger temperature step of 100 °C. It is important to note that any change in the surface of the as-prepared samples (LM, LCM, LSM and LBM), regarding oxygen/metal stoichiometry, will make these samples similar to the calcined ones (LM750, LCM750, LSM750 and LBM750 respectively). This surface modification may not be visible by X-ray powder diffraction, since this technique is more

sensitive to the bulk structure of the grains and not to the surface structure. However, Figure 2 shows that the as-prepared phases (exemplified for LSM) start showing indications of the transformation from orthorhombic to rhombohedral between 200 and 300 °C with change of oxygen content. We hypothesize, that the as-prepared, stoichiometric samples, show less activity than the calcined catalysts, but become quickly oxidized at the surface above 200 °C by the presence of O_2, making the activity of all the samples, above 200 °C equivalent among them, corresponding to the activity of the rhombohedral/cubic phases showing cation vacancies.

Only the determination of the Mn oxidation state at the surface may give a final answer to this hypothesis. XPS experiments are being planned for this purpose.

Table 2. Temperature values (°C) for conversions of 50 and 80% for the as-prepared and calcined samples.

Catalyst	T_{50} [°C]	T_{80} [°C]
LM	207	234
LM 750	200	231
LCM	225	246
LCM 750	196	233
LSM	227	258
LSM 750	182	223
LBM	219	241
LBM 750	196	231

Table 2 shows the temperature values for conversions of 50% (T_{50}) and 80% (T_{80}) of acetone. For all the compositions tested, there is a reduction in both temperatures with calcination. We hypothesize, again, that this increase in conversion activity is related to the presence of cation vacancies in the catalysts, as denounced by the observed rhombohedral LM750, LCM750 and LSM750 or rhombohedral/cubic LBM750 phases. The presence of metal vacancies would increase

the oxygen content of the sample facilitating oxygen mobility and surface exchange in a more defective surface that would not be favored in the as-prepared, stoichiometric samples with no vacancies.

4. Conclusions

Samples of as-prepared $LaMnO_3$, $La_{0.8}Ca_{0.2}MnO_3$, $La_{0.8}Sr_{0.2}MnO_3$ and $La_{0.8}Ba_{0.2}MnO_3$ (LM, LCM, LSM and LBM) and calcined at 750 °C $LaMnO_{3+\delta}$, $La_{0.8}Ca_{0.2}MnO_{3+\delta}$, $La_{0.8}Sr_{0.2}MnO_{3+\delta}$ and $La_{0.8}Ba_{0.2}MnO_{3+\delta}$ (LM750, LCM750, LSM750 and LBM750) have been prepared by an auto-combustion method, the crystal structure and surface area determined and tests for catalytic oxidation of acetone as a model VOC compound were performed. The results confirm that perovskite manganites have good catalytic activity for total oxidation of hydrocarbon compounds even showing low BET areas. Additionally, the change in oxygen stoichiometry caused by the formation of cation vacancies in the compounds favors the catalysis. The new preparation method of the perovskites may have an impact in reducing the costs of the catalyst preparation due to its simplicity. The change of AE seems to have a negligible effect on the catalytic properties, which again confirms that the bulk structure (mostly affected by AE ionic radii) has marginal influence on the catalysis, that seem more affected by Mn^{4+}/Mn^{3+} ratio in the surface than any other characteristic of the studied compounds. XPS experiments will be performed to confirm these conclusions.

5. Acknowledgements

6. References

[1] X. Zhang, B. Gao, A.E. Creamer et al. *J. Hazard Mat.* 338 (2017) 102-123.

[2] W.B. Li, J.X. Wang & H. Gong. *Catal. Today* 148 (2009) 81-87.

[3] M.S. Kamal, S.A. Razzak, M.M. Hossain. *Atmos. Environ.* 140 (2016) 117-134.

[4] R. Spinicci, M. Faticanti, P. Marini et al. *J. Mol. Catal. A-Chem.* 197 (2003) 147-155.

[5] J.M.D. Tascon & L. Gonzalez Tejuca. *J. Colloids Interfase Sci.* 102 (1984) 373-379.

[6] T. Arakawa, A. Yoshida, J. Shiokawa, *Mat. Res. Bull* 15 (1980) 269-273.

[7] S.C. Kim & W.G. Shim. *Appl. Catal. B-Environ.* 98 (2010) 180-185.

[8] B.P. Barbero, J.A. Gamboa & L.E. Cadús *Appl. Catal. B-Environ.* 65 (2006) 21-30.

[9] S. Vázquez, S. Davyt, J. F. Basbus, et al. *J. Solid State Chem.* 228 (2015) 208-213.

[10] B. Toby & R.B. Von Dreele. *J. Appl. Crystallogr.* 46(2) (2013) 544-549.

[11] G. H. Jonker & J. H. Van Santen. *Physica* 16(3) (1950) 337-349.

[12] A. Wold & R.J. Arnott, *J. Phys. Chem. Solids* 9 (1959) 176-180.

[13] J.A. Alonso, M.J. Martinez-Lope, M.T. Casais et al. *Solid State Commun.* 102 (1997) 7-12.

[14] J. Topfer & J. B. Goodenough. *J. Solid State Chem.* 130 (1997) 117-128.

[15] J.F. Mitchell, D.N. Argyriou, C.D. Potter et al. *Phys. Rev. B* 54(9) (1996) 6172-6183.

[16] R.H. Mitchell in *Perovskites, modern and ancient.* Almaz Press Inc. (2003) ISBN 13:978096841102.

[17] N. Rezlescu, E. Rezlescu, P.D. Popa. *Compos. Part B-Eng* 60 (2014) 545-522.

[18] K.L. Pan, G.T. Pan, S. Chong *J. Environ. Sci.* 69 (2018) 205-216.

[19] J. Yang, L. Li, X. Yang. *Catal. Today* 327 (2019) 19-27.

[20] R. Hammami, S.B. Aissa, H. Batis. *Appl. Catal. A-Gen* 353 (2009) 145-153.